

# Gait-based Recognition for Human Identification using Fuzzy Local Binary Patterns

Amer G. Binsaadoon and El-Sayed M. El-Alfy

*College of Computer Sciences and Engineering, King Fahd University of Petroleum and Minerals,  
Dhahran 31261, Saudi Arabia*

**Keywords:** Biometric, Human Identification, Gait Recognition, Local Binary Pattern, Fuzzy Logic.

**Abstract:** With the increasing security breaches nowadays, automated gait recognition has recently received increasing importance in video surveillance technology. In this paper, we propose a method for human identification at distance based on Fuzzy Local Binary Pattern (FLBP). After the Gait Energy Image (GEI) is generated as a spatiotemporal summary of a gait video sequence, a multi-region partitioning is applied and FLBP based features are extracted for each region. We also evaluate the performance under the variation of some factors including viewing angle, clothing and carrying conditions. The experimental work showed that GEI-FLBP with partitioning has remarkably enhanced the identification accuracy.

## 1 INTRODUCTION

Biometric technology has witnessed great advances in the past. However, common modalities such as face and fingerprint require controlled working conditions such as direct physical contact, closeness to acquisition devices, predefined views, and inevitable subject cooperation. Relatively recent, gait recognition has been shown to be an attractive alternative or complementary behavioral biometric. Gait is believed to have a unique pattern for each person in normal conditions. Moreover, it has the ability to mitigate the above mentioned requirements. It can have a feasible application in visual surveillance identification. Subjects are identified at distance (e.g. 10 m) based on the way they walk. Gait recognition doesn't require the subject under study to be close to the acquisition device or standing at a predefined viewing angle. In gait-based systems, subjects can be identified from low-resolution or infra-red images under different conditions such as wearing coats, carrying objects, or walking on different surfaces. A recent review of current techniques of gait recognition and modelling is present in (Lee et al., 2014).

Human identification approaches based on gait can be either model-based or model free. However, many of the research attempts are model-free due to the high computational cost and limited performance of model based methods (Zhang et al., 2010). Different model-free methods have been proposed in

the literature using various methods for feature extraction. One of the excellent methods for texture representation is local binary pattern (LBP), which was first proposed in 1996 by Ojala et al. (2002). It has been extensively utilized in a variety of research fields and has demonstrated notable performance (Brahnam et al., 2014). LBP has been used in face identification and expression recognition (Ahonen et al., 2006; Zhao and Pietikainen, 2007). A few attempts have been reported in the literature that utilize LBP for gait recognition. For example, Kellokumpu et al. (2009) proposed a new gait recognition method based on using LBP from Three Orthogonal Planes (LBP-TOP) that spatiotemporally represent the human movements. Hu et al. (2013) employed LBP to encode the motion flow information. In these two examples, only crisp LBP was used and was shown to be an effective texture representation. However, to cope with uncertainties that may result from noisy images, Iakovidis et al. (2008) incorporated fuzzy logic with LBP and named it FLBP.

In this work, we investigate the performance of applying fuzzy local binary patterns (FLBP) to extract more discriminative gait features from the Gait Energy Image (GEI) (Han and Bhanu, 2006a). GEI overcomes storage and computation burden of temporal model-free approaches by representing the human walking sequence in a single image conserving motion temporal properties. We also study the performance for different number of non-overlapping parti-

tions of GEI.

The remainder of this paper is organized as follows. Section 2 briefly reviews related work. Section 3 explains the proposed approach. Subsequently, experimental work on CASIA B gait dataset is discussed in Section 4. Finally, Section 5 concludes the paper.

## 2 RELATED WORK

Niyogi and Adelson (1994) presented an early attempt to model the image sequence of a person in spatiotemporal space dimensions. A model was fit on the extracted subject's contour and the model parameters were used for feature extraction. Lee and Grimson (2002) divided the original silhouette into seven parts, and extracted shape features consisting of ellipse fitting parameters of each region. Bhanu and Han (2002) estimated the human motion model parameters using a least-square fit to project the 3D kinematic motion into 2D silhouettes. Then, the estimated parameters were used to extract gait features.

On the other hand, model-free approaches (Ran et al., 2007; Ho et al., 2009; Zhang et al., 2010; Han and Bhanu, 2006a; Chen et al., 2010; Nizami et al., 2010) used static and dynamic components instead of fitting a model for the human motion. The static component reflects the shape and size of the person's body whereas the dynamic component reflects the movement dynamics. Examples of static features include height, width, stride length, and silhouette bounding box lengths. Frequency and phase of movement are examples of dynamic features.

Kale et al. (2003) proposed another algorithm to track the walker and extract his/her canonical pose. They used optical flow to discover the walking angle and then wrapping the image to the new canonical pose projection. The height and leg dynamics features were used. This resulted in encouraging recognition rate using the baseline algorithm of Sarkar et al. (2005).

Some other gait recognition approaches used the period of gait cycles as gait features. Ran et al. (2007) used two different methods to extract the period: Maximal Principal Gait Angle (MPGA) and the Fourier transform. They used the input and output signals generated by Voltage Controlled Oscillator (VCO) to get the cycle period as the phase difference of the two signals. Ho et al. (2009) used both static and dynamic features to determine the gait cycle period. Static features were the motion vector histograms and the dynamic features were the Fourier descriptors. They used Principal Component Analysis (PCA) and Multiple Discriminant Analysis to re-

duce the feature dimensionality. For the recognition process, they used the nearest neighbor classifier.

Kale et al. (2002) used the width vector feature analysis proposed in (Kale et al., 2004) to identify humans through their gaits. Width vector is the difference between the left and right boundaries in the binary silhouette representation space. As a classifier, they used Hidden Markov Model (HMM) for recognition. The main drawback of their approach is that it requires huge training data (more than 5,000 samples), which is not practical in gait application where the data is very limited. Moreover, HMM performance is sensitive to parameters initialization such as the number of states. Also, the viewing angle affects the overall recognition performance.

Zhang et al. (2010) proposed a new gait feature representation and called it Active Energy Image (AEI). AEI shows the actively moving regions. Successive frames are subtracted from each other and all differences are then summed and normalized. AEI reduces the effect of noise on the silhouette images. The authors applied two-dimensional Locality Preserving Projections (2D-LPP) to reduce dimensionality. They got high rate of recognition on the CASIA B dataset.

Wang et al. (2002) combined static and dynamic features to achieve high accuracy on the Soton gait database. The bidimensional silhouette was converted into unidimensional distance signal. For each silhouette, the distance from the origin into predefined points on the boundary of the silhouette was computed to represent the dynamic features. All distance signals were normalized using the magnitude and then exposed to eigen-based analysis for dimensionality reduction. Features like height and aspect ratios of the silhouette were used as static features and combined with the dynamic features to get the benefits of both. For recognition, a nearest neighbor technique was used.

Lee (2001) divided the binary silhouette of a walking human into seven elliptical-shaped regions. The walking person was perpendicular to the image plane. View and appearance based approach was used to transform the person image into the image plane. Features were extracted from the seven ellipses in form of parameters. However, the parameters were exposed to noise and it was difficult to find the periodicity using these features. As an efficient solution, mean and standard deviation of the features were computed to be used as the final summary features.

Han and Bhanu (2006a) proposed a new effective method to summarize the silhouette sequence spatiotemporally into a Gait Energy Image (GEI). Gait cycle was extracted from the gait sequence of silhouette and then all involved frames were summed and

normalized to get the GEI image. GEI describes how motion proceeds and which regions are more involved in motion, the brighter it is in the GEI image. Several gait recognition approaches relied on features extracted from GEIs (Li et al., 2012; Huang et al., 2013; Wang et al., 2014; Mansur et al., 2014). However, they used reduced-dimensionality GEIs or applied the feature extraction algorithm on the holistic GEI.

Chen et al. (2010) proposed a dimensionality reduction method called tensor-based Riemannian manifold distance-approximating projection (TRIMAP). A graph was constructed from the given data in a way that preserves the geodesic distance between data points. Then, the graph was projected into a lower dimensional space by tensor-based optimization methods. The authors used Gabor filter to extract features from GEI representation of gait image sequences and applied their dimensionality reduction on the extracted features.

Nizami et al. (2010) divided the whole gait sequence into subsets and derived their own summarization method called Moving Motion Silhouette Images (MMSI) for each subset. Independent Component Analysis (ICA) was used for dimensionality reduction purpose. Probabilistic Support Vector Machine (SVM) was used to classify the independent components. They evaluated the method on CASIA A and SotonBig datasets.

Abdelkader (2002) tracked the walker in video surveillance using bounding boxes. The frequency of walking and stride length were then extracted through these bounding boxes. To reduce the effect of the pose of the walker, the height was included as a feature as well. The recognition rate was 51% and enhanced to 65% using 2-dimensional and 4-dimensional feature vectors respectively.

Lu and Zhang (2007) proposed a fusion strategy to improve the classification performance in gait-based human identification. Three features were used: Fourier descriptor, wavelet descriptor, and pseudo-Zernike moment. First, the silhouettes were extracted and binarized. Then, the three types of features were extracted from the binary silhouettes and ICA was used for dimensionality reduction. The authors performed the fusion on the decision level not the feature level. The match scores for each feature in each view were fused using the product of sum fusion strategy. Genetic fuzzy SVM (GFSVM) was used as the classifier. The experiments were conducted on CASIA A (20 subjects) and AUXT (50 subjects) datasets. Each subject has 3 different views and 4 sequences in each view. They achieved 95% recognition rate.

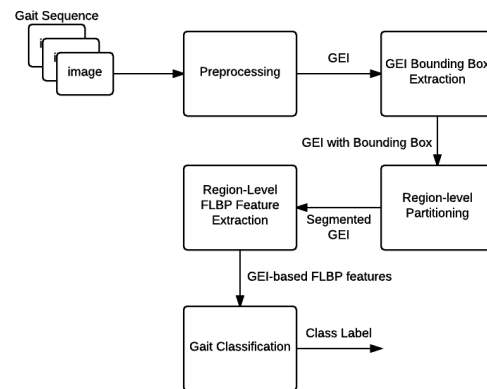


Figure 1: Gait recognition framework.

### 3 METHODOLOGY

In this section, we describe the proposed methodology for gait recognition. Figure 1 shows an outline of the proposed framework. Our approach is based on the generation of GEI and applying FLBP to extract effective features. However, unlike earlier GEI-based approaches for gait recognition, which mainly utilize the holistic GEI image, our approach applies FLBP feature extraction in non-overlapped regions.

#### 3.1 Motion Sequence Representation

Human silhouettes are extracted for various motion frames by background subtraction and thresholding, shadow elimination, morphological postprocessing and normalization. GEI image is then calculated to represent the motion sequence of a particular cycle in a single image while preserving the temporal information. The formula to calculate GEI is as follows (Han and Bhanu, 2006b):

$$G(x, y) = \frac{1}{M} \sum_{t=1}^N B(x, y, t) \quad (1)$$

where  $M$  is the number of frames in a complete cycle in the silhouette sequence,  $x$  and  $y$  are the spatial coordinate, and  $B(x, y, t)$  is the binary silhouette of the  $t$ -th frame.

#### 3.2 Feature Extraction

##### 3.2.1 Crisp Local Binary Patterns (LBP)

The crisp form of local binary patterns uses the properties of the neighborhood pixels to describe each pixel. It is computationally simple, efficient, resistant to gray level changes made by lighting variations. It

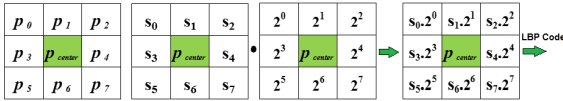


Figure 2: An example of LBP computation.

has the ability to capture fine texture details. The main idea behind LBP is to extract the local micropatterns in an image and to describe their distribution through a histogram (in our case we used 256 bins). Each pixel in the image  $p_{center}$  is compared to its neighboring pixels  $p_i$  and an LBP code is computed as follows (Brahnam et al., 2014):

$$LBP_{center} = \sum_{i=0}^{N-1} s(p_i - p_{center}) 2^i \quad (2)$$

where  $N$  is the number of neighboring pixels and  $s(x)$  is an indicator function such that  $s(x) = 1$  if  $x \geq 0$  and  $s(x) = 0$  otherwise. After passing the operator over the whole image or block, a 256-bin histogram of the binary patterns is constructed to be used as the feature vector. Figure 2 shows an illustrative example of LBP computation with  $N = 8$ .

Despite the good characteristics of crisp LBP in representing textures, it cannot handle all the machine learning related problems. It uses hard thresholding in computing its code and thus is more sensitive to noise and has less discrimination power. Also, the classifiers used directly affect the performance.

### 3.2.2 Fuzzy Local Binary Patterns (FLBP)

Fuzzy LBP (FLBP) (Iakovidis et al., 2008) incorporates fuzzy logic with LBP in order to alleviate the effect of noise on LBP and increase its distinguishing capability. The difference between crisp LBP and Fuzzy LBP is that in FLBP each pixel can be characterized by more than one LBP code which in turn contributes in more than one bin of FLBP histogram.

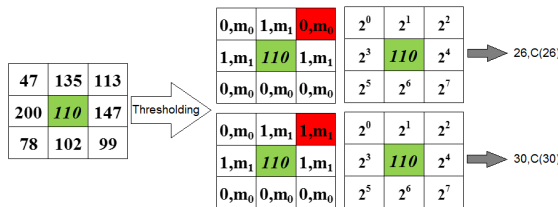


Figure 3: An example of FLBP computation.

An example of FLBP computation is shown in Figure 3. Two membership functions are computed  $m_1()$  and  $m_0()$  which indicate to what extent a neighboring pixel  $p_i$  has a greater or smaller gray value than  $p_{center}$ , respectively.  $T$  is the threshold parameter that

controls the degree of fuzziness. In our experiments,  $T$  is set to 5. The calculations of membership functions are as follows:

$$m_0(i) = \begin{cases} 0 & p_i \geq p_{center} + T \\ \frac{T - p_i + p_{center}}{2T} & p_{center} - T < p_i < p_{center} + T \\ 1 & p_i \leq p_{center} - T \end{cases} \quad (3)$$

$$m_1(i) = 1 - m_0(i) \quad (4)$$

Unlike LBP, each  $3 \times 3$  neighborhood can be characterized by more than one LBP code. The membership functions  $m_1()$  and  $m_0()$  are used to determine the contribution of each LBP code to a single bin of the FLBP histogram. The contribution of each LBP is defined as follows:

$$C(LBP) = \prod_{i=0}^8 m_{s_i}(i) \quad (5)$$

where  $s_i \in \{0, 1\}$ . The sum of all contributions of a single  $3 \times 3$  neighborhood is always equal to unity as follows:

$$\sum_{LBP=0}^{255} C(LBP) = 1 \quad (6)$$

Crisp LBP histograms may have bins of zero value. However, FLBP histograms have no zero-valued bins and thus are more informative than the crisp LBP.

### 3.3 Partitioning

First, GEI bounding box is automatically extracted as a preprocessing step as illustrated left side of Figure 4. To enhance the performance of FLBP features, we explored partitioning the GEI into different-sized non-overlapping predefined regions. The partitioning has been conducted as a fraction of the subject's height and width and denoted by horizontal and vertical lines. The underlying idea is to separate moving parts such as head, arms, legs, etc. After normalization and alignment of GEI, we statically set the boundaries between regions. For example, we set the head part to include about 19% of the whole subject's height. Figure 4 shows two examples of non-overlapping partitioning into 7 and 5 regions. Different partitioning scenarios are evaluated in our experiments.

### 3.4 Gait Classification

In this stage, a support vector machine (SVM) classifier with a linear kernel is used for gait recognition using the extracted feature vectors. There are several

Table 1: Performance comparison of LBP and FLBP under *Normal-Walking* covariate without partitioning.

| Angle(°) | LBP         |             |           |       | FLBP        |             |           |       |
|----------|-------------|-------------|-----------|-------|-------------|-------------|-----------|-------|
|          | $PRE_{avg}$ | $REC_{avg}$ | $F_{avg}$ | $ACC$ | $PRE_{avg}$ | $REC_{avg}$ | $F_{avg}$ | $ACC$ |
| 0        | 54.00       | 56.00       | 52.00     | 56.90 | 75.00       | 74.00       | 72.00     | 74.14 |
| 18       | 68.00       | 66.00       | 64.00     | 66.81 | 79.00       | 78.00       | 76.00     | 78.45 |
| 36       | 60.00       | 60.00       | 57.00     | 60.35 | 69.00       | 67.00       | 65.00     | 67.24 |
| 54       | 56.00       | 56.00       | 53.00     | 56.90 | 74.00       | 74.00       | 71.00     | 74.14 |
| 72       | 70.00       | 68.00       | 67.00     | 68.54 | 74.00       | 75.00       | 73.00     | 75.43 |
| 90       | 72.00       | 73.00       | 70.00     | 73.28 | 79.00       | 78.00       | 76.00     | 78.02 |
| 108      | 68.00       | 69.00       | 66.00     | 68.97 | 75.00       | 76.00       | 73.00     | 76.29 |
| 126      | 62.00       | 62.00       | 60.00     | 62.50 | 77.00       | 76.00       | 74.00     | 75.86 |
| 144      | 62.00       | 61.00       | 58.00     | 61.21 | 76.00       | 75.00       | 73.00     | 75.00 |
| 162      | 67.00       | 69.00       | 65.00     | 68.97 | 80.00       | 78.00       | 76.00     | 77.59 |
| 180      | 54.00       | 57.00       | 52.00     | 57.33 | 73.00       | 71.00       | 70.00     | 70.69 |
| Avg.     | 63.00       | 63.36       | 60.36     | 63.80 | 75.55       | 74.73       | 72.64     | 74.80 |

Table 2: Performance comparison of LBP and FLBP under *Carrying-Bag* covariate without partitioning.

| Angle(°) | LBP         |             |           |       | FLBP        |             |           |       |
|----------|-------------|-------------|-----------|-------|-------------|-------------|-----------|-------|
|          | $PRE_{avg}$ | $REC_{avg}$ | $F_{avg}$ | $ACC$ | $PRE_{avg}$ | $REC_{avg}$ | $F_{avg}$ | $ACC$ |
| 0        | 24.00       | 28.00       | 23.00     | 28.02 | 38.00       | 40.00       | 36.00     | 40.85 |
| 18       | 43.00       | 43.00       | 40.00     | 43.10 | 43.00       | 43.00       | 39.00     | 43.54 |
| 36       | 33.00       | 34.00       | 31.00     | 34.05 | 28.00       | 35.00       | 30.00     | 36.91 |
| 54       | 29.00       | 30.00       | 27.00     | 30.60 | 30.00       | 34.00       | 29.00     | 33.62 |
| 72       | 34.00       | 34.00       | 30.00     | 34.05 | 28.00       | 35.00       | 30.00     | 36.72 |
| 90       | 35.00       | 37.00       | 34.00     | 37.50 | 38.00       | 40.00       | 36.00     | 40.10 |
| 108      | 32.00       | 34.00       | 30.00     | 34.48 | 33.00       | 38.00       | 33.00     | 38.90 |
| 126      | 31.00       | 31.00       | 28.00     | 31.47 | 31.00       | 31.00       | 28.00     | 31.16 |
| 144      | 25.00       | 28.00       | 24.00     | 28.02 | 26.00       | 31.00       | 26.00     | 30.16 |
| 162      | 33.00       | 35.00       | 31.00     | 35.35 | 38.00       | 40.00       | 36.00     | 40.55 |
| 180      | 27.00       | 29.00       | 25.00     | 29.74 | 33.00       | 38.00       | 33.00     | 37.35 |
| Avg.     | 31.45       | 33.00       | 29.36     | 33.31 | 33.27       | 36.82       | 32.36     | 37.26 |

Table 3: Performance comparison of LBP and FLBP under *Wearing-Coat* covariate without partitioning.

| Angle(°) | LBP         |             |           |       | FLBP        |             |           |       |
|----------|-------------|-------------|-----------|-------|-------------|-------------|-----------|-------|
|          | $PRE_{avg}$ | $REC_{avg}$ | $F_{avg}$ | $ACC$ | $PRE_{avg}$ | $REC_{avg}$ | $F_{avg}$ | $ACC$ |
| 0        | 7.00        | 9.00        | 7.00      | 9.91  | 8.00        | 11.00       | 8.00      | 11.33 |
| 18       | 7.00        | 9.00        | 7.00      | 9.91  | 14.00       | 16.00       | 13.00     | 16.50 |
| 36       | 13.00       | 15.00       | 13.00     | 15.95 | 16.00       | 18.00       | 14.00     | 17.62 |
| 54       | 16.00       | 18.00       | 15.00     | 18.10 | 17.00       | 20.00       | 17.00     | 20.64 |
| 72       | 11.00       | 16.00       | 12.00     | 16.38 | 17.00       | 20.00       | 17.00     | 20.36 |
| 90       | 12.00       | 15.00       | 12.00     | 15.09 | 18.00       | 21.00       | 17.00     | 21.07 |
| 108      | 10.00       | 13.00       | 10.00     | 13.79 | 14.00       | 16.00       | 13.00     | 16.50 |
| 126      | 14.00       | 17.00       | 14.00     | 17.24 | 16.00       | 18.00       | 14.00     | 18.52 |
| 144      | 9.00        | 10.00       | 8.00      | 10.78 | 10.00       | 14.00       | 10.00     | 14.81 |
| 162      | 7.00        | 10.00       | 6.00      | 10.78 | 11.00       | 13.00       | 11.00     | 13.91 |
| 180      | 8.00        | 11.00       | 8.00      | 11.21 | 11.00       | 13.00       | 11.00     | 13.91 |
| Avg.     | 10.36       | 13.00       | 10.18     | 13.56 | 13.82       | 16.36       | 13.18     | 16.83 |

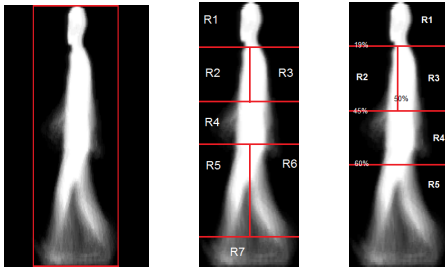


Figure 4: Bounding box and two examples of non-overlapping partitioning of GEI with 7 and 5 regions.

implementations of SVM. In our study, we built our model using LibSVM which implements one-against-one for multi-class classification. If  $k$  is the number of subjects under investigation, then  $k(k-1)/2$  binary classifiers are constructed. Each classifier is trained on data belonging to two classes. Then max-win voting scheme is used to decide the predicted class. If there is a tie (more than one class has identical max vote, the one with the smaller index is chosen). We could also use one-versus-all, but based on the comparisons conducted in (Hsu and Lin, 2002), the one-versus-one training time was shorter with high accuracy.

## 4 EVALUATION

### 4.1 Dataset

The proposed approach is evaluated on CASIA B; which is a large multiview gait database maintained by the Institute of Automation, Chinese Academy of Sciences (Yu et al., 2006). It includes sequence samples of 124 subjects of 93 males and 31 females. Gait sequences for each subject were captured from 11 different views in an indoor environment with simple background. Each subject was asked to walk 10 times through a straight line of concrete ground (6 normal walking, 2 wearing a coat, 2 carrying a bag). At each walking, there were 11 cameras capturing the subject walking. Consequently, each subject has 110 video sequences and the database contains  $110 \times 124 = 13640$  total video sequences for all subjects.

### 4.2 Performance Measures

We used four measures to evaluate and compare the performance of gait recognitions based on LBP and FLBP. These measures are: accuracy, precision, recall and  $F$ -measure. The accuracy is calculated as

follows:

$$ACC = \frac{\sum_{i=1}^S TP_i}{\sum_{i=1}^S (TP_i + FN_i)} \quad (7)$$

where  $S$  is the number of classes (i.e. subjects),  $TP_i$  is the number of subjects that are correctly predicted to be of class  $i$ , and  $TN_i$  is the number of subjects of class  $i$  that are incorrectly predicted to be of other classes. The precision measures the relevancy of results. In other words, it is the fraction of relevant retrieved instances. High value of precision indicates a low false positive rate and shows that the classifier and features are more accurate. We used the average precision for all subjects which is defined as follows:

$$PRE_{avg} = \frac{1}{S} \sum_{i=1}^S \frac{TP_i}{(TP_i + FP_i)} \quad (8)$$

The recall measures how many relevant instances are correctly retrieved. High value of recall indicates a low false negative rate and shows that the classifier is returning the majority of the positive instances. We used the average precision for all subjects which is defined as follows:

$$REC_{avg} = \frac{1}{S} \sum_{i=1}^S \frac{TP_i}{(TP_i + FN_i)} \quad (9)$$

The  $F$ -measure is the harmonic mean of precision and recall for each class. Then we used the average  $F$ -measure as given by:

$$F_{avg} = \frac{1}{S} \sum_{i=1}^S \left\{ 2 \cdot \frac{PRE_i \times REC_i}{(PRE_i + REC_i)} \right\} \quad (10)$$

where  $PRE_i$  and  $REC_i$  are the precision and recall for class  $i$ , respectively.

Table 4: Comparison of recognition rates under *Normal-Walking* with different *non-overlapping* partitioning.

| Angle(°) | Number of Regions |       |       |       |       |
|----------|-------------------|-------|-------|-------|-------|
|          | Holistic          | 5     | 7     | 8     | 10    |
| 0        | 74.14             | 96.55 | 97.41 | 98.71 | 98.71 |
| 18       | 78.45             | 96.98 | 97.85 | 98.71 | 98.28 |
| 36       | 67.24             | 92.67 | 94.83 | 96.12 | 95.26 |
| 54       | 74.14             | 95.69 | 95.69 | 97.41 | 98.28 |
| 72       | 75.43             | 94.4  | 94.83 | 96.55 | 97.41 |
| 90       | 78.02             | 92.67 | 94.4  | 95.26 | 95.69 |
| 108      | 76.29             | 96.55 | 96.12 | 97.85 | 97.85 |
| 126      | 75.86             | 95.26 | 96.55 | 96.98 | 96.55 |
| 144      | 75                | 96.55 | 96.12 | 96.55 | 97.41 |
| 162      | 77.59             | 96.55 | 98.28 | 97.41 | 98.28 |
| 180      | 70.69             | 96.12 | 98.28 | 99.14 | 99.14 |
| Avg.     | 74.80             | 95.45 | 96.40 | 97.34 | 97.53 |

### 4.3 Results and Discussion

The performance of our proposed approach is evaluated under different environmental conditions using Matlab implementation. The experiments setup is similar to the one adopted by the authors of CASIA

B database (Yu et al., 2006). The gallery set of normal walking of all subjects is always used to train the SVM model. Three sets under different covariates are used as the probe sets as follows: normal walking, carrying bag, and wearing coat. Sequences of subjects under normal walking were chosen to be the gallery set as proposed by the authors of CASIA B dataset. Probe sets are taken in three different covariates: walking normally, carrying bag, and wearing coat.

First, the proposed approach was applied on the GEI without any partitioning. Then, FLBP is applied and compared with LBP. All comparisons were conducted in terms of recognition rates (accuracy), precision, recall and  $F$ -measure. As shown in Tables 1, 2, and 3, FLBP-based features have better accuracy for each covariate.

To evaluate the effect of partitioning on the recognition rate, a group of experiments is designed. The results are shown in Tables 4, 5, and 6 for three different scenarios. These results demonstrate that using the holistic image has lower performance. Moreover, it is clear that more partitions lead to enhanced results. However, it is not a guarantee that with this number of partitions we can always get the best performance in all cases.

## 5 CONCLUSIONS

In this paper, a fuzzy version of LBP was investigated and applied for gait recognition. The GEIs images of CASIA B dataset were partitioned into non-overlapping regions. Then, we investigated FLBP operator to extract more local discriminative gait features. The experimental results showed that the proposed framework is outperforming LBP. Moreover, the results demonstrated that using partitioning can enhance the performance to promising levels. Future work can include the investigation of FLBP on other gait datasets and representations.

Table 5: Comparison of recognition rates under *Carrying-Bag* with different *non-overlapping* partitioning.

| Angle(°) | Number of Regions |       |       |       |       |
|----------|-------------------|-------|-------|-------|-------|
|          | Holistic          | 5     | 7     | 8     | 10    |
| 0        | 40.85             | 62.5  | 69.4  | 72.85 | 73.71 |
| 18       | 43.54             | 48.71 | 52.16 | 60.78 | 58.19 |
| 36       | 36.91             | 44.4  | 49.14 | 48.71 | 50.43 |
| 54       | 33.62             | 33.19 | 35.35 | 43.54 | 40.95 |
| 72       | 36.72             | 31.9  | 34.91 | 35.35 | 35.78 |
| 90       | 40.1              | 36.21 | 42.24 | 34.05 | 35.35 |
| 108      | 38.9              | 32.76 | 38.79 | 25.86 | 30.17 |
| 126      | 31.16             | 35.35 | 36.64 | 36.64 | 37.08 |
| 144      | 30.16             | 40.52 | 48.71 | 41.38 | 45.26 |
| 162      | 40.55             | 59.91 | 63.36 | 65.09 | 63.79 |
| 180      | 37.35             | 62.07 | 66.81 | 65.95 | 68.97 |
| Avg.     | 37.26             | 44.32 | 48.86 | 48.2  | 49.06 |

Table 6: Comparison of recognition rates under *Wearing-Coat* with different *non-overlapping* partitioning.

| Angle(°) | Number of Regions |       |       |       |       |
|----------|-------------------|-------|-------|-------|-------|
|          | Holistic          | 5     | 7     | 8     | 10    |
| 0        | 11.33             | 19.83 | 23.71 | 34.91 | 33.62 |
| 18       | 16.5              | 27.16 | 31.47 | 35.78 | 34.48 |
| 36       | 17.62             | 22.41 | 26.72 | 36.64 | 33.19 |
| 54       | 20.64             | 25.86 | 31.04 | 40.52 | 43    |
| 72       | 20.36             | 28.45 | 31.9  | 34.91 | 34    |
| 90       | 21.07             | 28.88 | 33.62 | 41.38 | 41.81 |
| 108      | 16.5              | 29.31 | 37.93 | 36.21 | 38.36 |
| 126      | 18.52             | 22.41 | 27.16 | 37.5  | 35.35 |
| 144      | 14.81             | 25.43 | 27.16 | 37.07 | 36.64 |
| 162      | 13.91             | 33.62 | 34.48 | 37.5  | 37.93 |
| 180      | 13.9              | 31.04 | 38.79 | 39.22 | 39.22 |
| Avg.     | 16.83             | 26.76 | 31.27 | 37.42 | 37.05 |

## ACKNOWLEDGEMENT

The authors would like to thank King Fahd University for Petroleum and Minerals (KFUPM), and Hadhramout Establishment for Human Development for their support during this work.

## REFERENCES

- Abdelkader, C. B. (2002). Stride and cadence as a biometric in automatic person identification and verification. In *Proc. 5th IEEE International Conf. on Automatic Face and Gesture Recognition*.
- Ahonen, T., Hadid, A., and Pietikainen, M. (2006). Face description with local binary patterns: Application to face recognition. *IEEE Transactions on Pattern Analysis and Machine Intelligence*, 28(12):2037–2041.
- Bhanu, B. and Han, J. (2002). Individual recognition by kinematic-based gait analysis. In *Proceedings of 16th International Conference on Pattern Recognition*.
- Brahnam, S., Jain, L. C., Nanni, L., and Lumini, A. (2014). *Local Binary Patterns - New Variants and Applications*. Springer-Verlag Berlin Heidelberg 2014.
- Chen, C., Zhang, J., and Fleischer, R. (2010). Distance approximating dimension reduction of riemannian manifolds. *IEEE Transactions on Systems, Man, and Cybernetics, Part B: Cybernetics*, 40(1):208–217.
- Han, J. and Bhanu, B. (2006a). Individual recognition using gait energy image. *IEEE Transactions on Pattern Analysis and Machine Intelligence*, 28(2):316–322.
- Han, J. and Bhanu, B. (2006b). Individual recognition using gait energy image. *IEEE Trans. Pattern Analysis and Machine Intelligence*, 28(2):316–322.
- Ho, M.-F., Chen, K.-Z., and Huang, C.-L. (2009). Gait analysis for human walking paths and identities recognition. In *IEEE International Conference on Multimedia and Expo (ICME)*.
- Hsu, C.-W. and Lin, C.-J. (2002). A comparison of methods for multiclass support vector machines. *IEEE Trans. Neural Networks*, 13(2):415–425.

- Hu, M., Wang, Y., Zhang, Z., Zhang, D., and Little, J. (2013). Incremental learning for video-based gait recognition with lbp flow. *IEEE Transactions on Cybernetics*, 43(1):77–89.
- Huang, D.-Y., Lin, T.-W., Hu, W.-C., and Cheng, C.-H. (2013). Gait recognition based on gabor wavelets and modified gait energy image for human identification. *Journal of Electronic Imaging*, 22(4).
- Iakovidis, D., Keramidas, E., and Maroulis, D. (2008). Fuzzy local binary patterns for ultrasound texture characterization. In Campilho, A. and Kamel, M., editors, *Image Analysis and Recognition*, volume 5112 of *Lecture Notes in Computer Science*, pages 750–759. Springer Berlin Heidelberg.
- Kale, A., Chowdhury, A., and Chellappa, R. (2003). Towards a view invariant gait recognition algorithm. In *Proceedings of IEEE Conference on Advanced Video and Signal Based Surveillance*.
- Kale, A., Rajagopalan, A., Cuntoor, N., and Kruger, V. (2002). Gait-based recognition of humans using continuous hmms. In *Proc. 5th IEEE International Conf. on Automatic Face and Gesture Recognition*.
- Kale, A., Sundaresan, A., Rajagopalan, A., Cuntoor, N., Roy-Chowdhury, A., Kruger, V., and Chellappa, R. (2004). Identification of humans using gait. *IEEE Transactions on Image Processing*, 13(9):1163–1173.
- Kellokumpu, V., Zhao, G., Li, S., and Pietikäinen, M. (2009). Dynamic texture based gait recognition. In *Advances in Biometrics*, volume 5558 of *Lecture Notes in Computer Science*. Springer Berlin Heidelberg.
- Lee, L. (2001). Gait dynamics for recognition and classification. In *Proceedings of the 5th IEEE International Conference on Automatic Face and Gesture Recognition (AFGR)*.
- Lee, L. and Grimson, W. (2002). Gait analysis for recognition and classification. In *Proceedings of Fifth IEEE International Conference on Automatic Face and Gesture Recognition*, pages 148–155.
- Lee, T. K. M., Belkhatir, M., and Sanei, S. (2014). A comprehensive review of past and present vision-based techniques for gait recognition. *Multimedia Tools and Applications*, 72(3):2833–2869.
- Li, C.-R., Li, J.-P., Yang, X.-C., and Liang, Z.-W. (2012). Gait recognition using the magnitude and phase of quaternion wavelet transform. In *International Conference on Wavelet Active Media Technology and Information Processing (ICWAMTIP)*.
- Lu, J. and Zhang, E. (2007). Gait recognition for human identification based on {ICA} and fuzzy {SVM} through multiple views fusion. *Pattern Recognition Letters*, 28(16):2401 – 2411.
- Mansur, A., Makihara, Y., Muramatsu, D., and Yagi, Y. (2014). Cross-view gait recognition using view-dependent discriminative analysis. In *IEEE International Joint Conference on Biometrics (IJCB)*.
- Niyogi, S. and Adelson, E. (1994). Analyzing and recognizing walking figures in xyt. In *Proceedings of IEEE Computer Society Conference on Computer Vision and Pattern Recognition*, pages 469–474.
- Nizami, I. F., Hong, S., Lee, H., Lee, B., and Kim, E. (2010). Automatic gait recognition based on probabilistic approach. *International Journal of Imaging Systems and Technology*, 20(4):400–408.
- Ojala, T., Pietikainen, M., and Maenpaa, T. (2002). Multiresolution gray-scale and rotation invariant texture classification with local binary patterns. *IEEE Transactions on Pattern Analysis and Machine Intelligence*, 24(7):971–987.
- Ran, Y., Weiss, I., Zheng, Q., and Davis, L. (2007). Pedestrian detection via periodic motion analysis. *International Journal of Computer Vision*, 71(2).
- Sarkar, S., Phillips, P., Liu, Z., Vega, I., Grother, P., and Bowyer, K. (2005). The humanid gait challenge problem: data sets, performance, and analysis. *IEEE Transactions on Pattern Analysis and Machine Intelligence*, 27(2):162–177.
- Wang, K., Xing, X., Yan, T., and Lv, Z. (2014). Couple metric learning based on separable criteria with its application in cross-view gait recognition. In *Biometric Recognition*, volume 8833 of *Springer Lecture Notes in Computer Science*, pages 347–356.
- Wang, L., Hu, W., and Tan, T. (2002). A new attempt to gait-based human identification. In *Proc. 16th International Conference on Pattern Recognition*.
- Yu, S., Tan, D., and Tan, T. (2006). A framework for evaluating the effect of view angle, clothing and carrying condition on gait recognition. In *Proc. 18th International Conf. on Pattern Recognition*, volume 4, pages 441–444.
- Zhang, E., Zhao, Y., and Xiong, W. (2010). Active energy image plus 2dlpp for gait recognition. *Signal Processing*, 90(7):2295 – 2302.
- Zhao, G. and Pietikainen, M. (2007). Dynamic texture recognition using local binary patterns with an application to facial expressions. *IEEE Transactions on Pattern Analysis and Machine Intelligence*, 29(6):915–928.